Centriole maturation requires regulated Plk1 activity during two consecutive cell cycles

Dong Kong, Veronica Farmer, Anil Shukla, Jana James, Richard Gruskin, Shigeo Kiriyama, and Jadranka Loncarek

Laboratory of Protein Dynamics and Signaling, Center for Cancer Research–Frederick, National Cancer Institute, National Institutes of Health, Frederick, MD 21702

Newly formed centrioles in cycling cells undergo a maturation process that is almost two cell cycles long before they become competent to function as microtubule-organizing centers and basal bodies. As a result, each cell contains three generations of centrioles, only one of which is able to form cilia. It is not known how this long and complex process is regulated. We show that controlled Plk1 activity is required for gradual biochemical and structural maturation of the centrioles and timely appendage assembly. Inhibition of Plk1 impeded accumulation of appendage proteins and appendage formation. Unscheduled Plk1 activity, either in cycling or interphase-arrested cells, accelerated centriole maturation and appendage and cilia formation on the nascent centrioles, erasing the age difference between centrioles in one cell. These findings provide a new understanding of how the centriole cycle is regulated and how proper cilia and centrosome numbers are maintained in the cells.

Introduction

Centriole duplication cycle controls centrosome number by synchronizing the formation of new centrioles with the DNA replication cycle. Two resident mother centrioles (MCs) duplicate at the beginning of S phase by each forming one daughter centriole (DC) in an orthogonal orientation (Robbins et al., 1968; Rattner and Phillips, 1973; Vorobjev and Chentsov, 1982), which elongates throughout S and G2. The resolution of orthogonal orientation–centriole disengagement (Vidwans et al., 1999; Tsou and Stearns, 2006) occurs by the end of mitosis, and afterward, two centrioles organize independent centrosomes. After initiation of their formation, DCs undergo a series of biochemical and structural modifications needed to acquire a competence for pericentriolar material (PCM) organization, duplication, and cilia assembly (Hoyer-Fender, 2010). This ill-understood centriole maturation process is almost two cell cycles long, and as a consequence, each cycling cell contains three generations of centrioles. Only one centriole per cell (the oldest one) is fully structurally mature and decorated with subdistal and distal appendages (Vorobjev and Chentsov, 1982; Paintrand et al., 1992), which are needed for microtubule anchoring during interphase and for ciliogenesis, respectively (Mogensen et al., 2000; Nakagawa et al., 2001; Hoyer-Fender, 2010; Tateishi et al., 2013). Appendages first form on the centriole by the end of its second mitosis (Robbins et al., 1968; Vorobjev and Chentsov, 1982), well after the centriole has already acquired its full length, organized a PCM, and undergone duplication in the previous cell cycle. Mechanisms that regulate appendage formation remain elusive.

Mitotic kinase Plk1 (Polo-like kinase 1) is required for centriole disengagement in mitosis (Tsou et al., 2009) and during interphase arrest (Lončarek et al., 2010). In our previous work, we demonstrated that expression of active Plk1 induces accumulation of subdistal appendage protein Cep170 (Guarguaglini et al., 2005) on disengaged DCs during S phase (Lončarek et al., 2010), indicating that Plk1 might be involved in formation of centriole appendages.

Here, we investigate the effects of Plk1 on biochemical and structural centriole maturation, focusing on two less-characterized hallmarks of that process: centriole elongation and appendage assembly. Our analysis revealed that Plk1 promotes elongation of DCs in S-arrested and cycling cells. Furthermore, we found that exogenous expression of Plk1 stimulates premature accumulation of appendage proteins Cep164, Odf2/Cenexin, FBF1, SCLT1, and ccdc41 and assembly of

Correspondence to Jadranka Loncarek: jadranka.loncarek@nih.gov

J. James's present address is Women's Malignancies Branch, National Cancer Institute, National Institutes of Health, Bethesda, MD 20892.

R. Gruskin and Shigeo Kiriyama's present address is Software Systems Dept., Nikon, Melville, NY 11747.

Abbreviations used in this paper: CLEM, correlative light and EM; DC, daughter centriole; dox, doxycycline; HU, hydroxyurea; MC, mother centriole; PCM, pericentriolar material; TIRF, total internal reflection fluorescence.

The Rockefeller University Press $30.00
J. Cell Biol. Vol. 206 No. 7 855–865
www.jcb.org/cgi/doi/10.1083/jcb.201407087

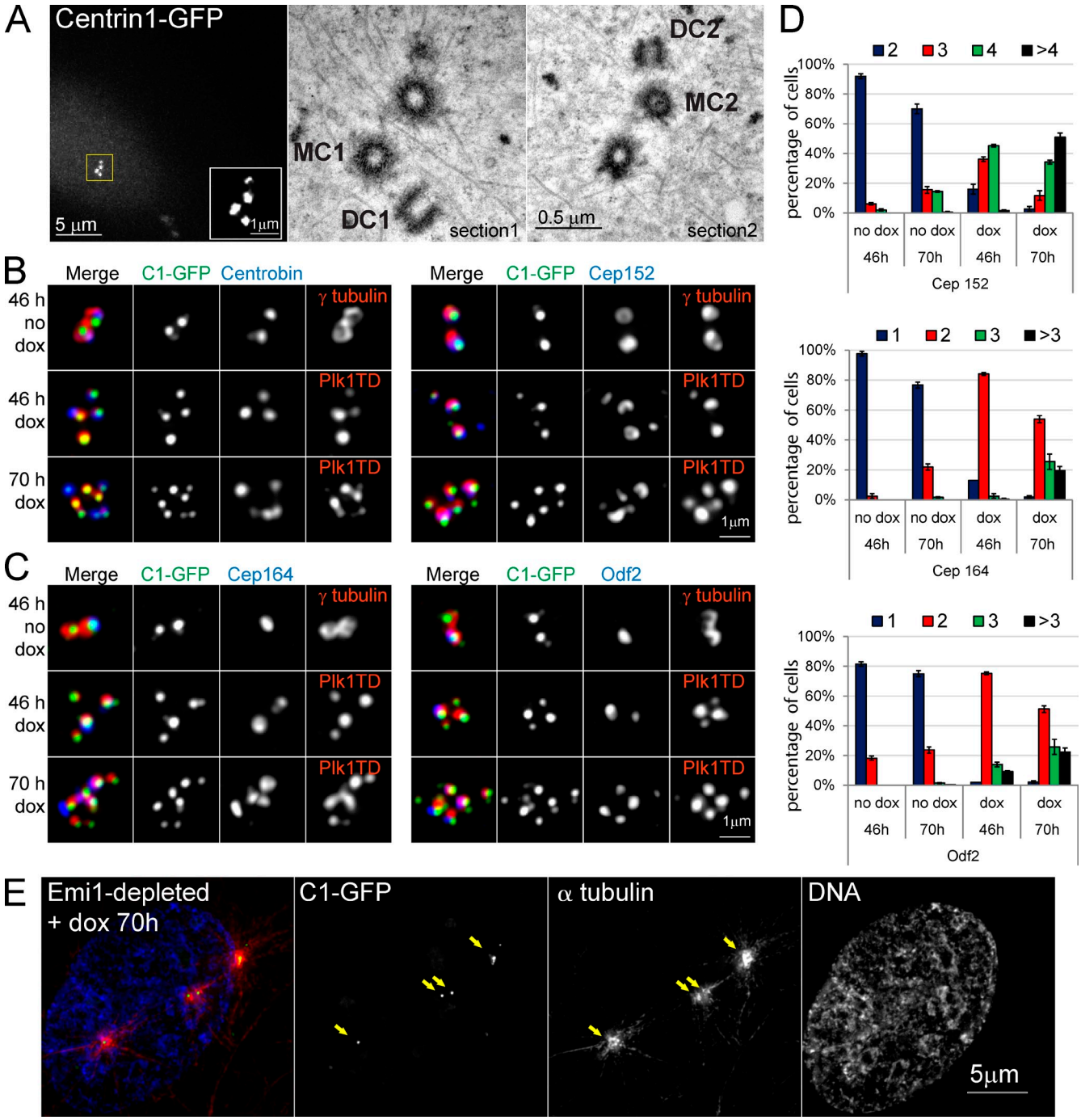

Figure 1. **Expression of Plk1TD in Emi1-d U2OS cells induces disengagement of short procentrioles that gradually biochemically mature.** (A) EM analysis of an Emi1-d Plk1TD-expressing U2OS cell with newly disengaged DCs. Four C1-GFP signals indicate the presence of four centrioles. EM analysis of the same centrioles reveals two longitudinally sectioned DCs (~260 nm DC1 and ~220 nm DC2) in the vicinity of two MCs in cross section. (B and C) Localization of Centrobin, Cep152, Cep164, and Odf2 on the centrioles of Emi1-d cells, with or without Plk1TD expression. (D) Quantification of the data presented in B and C. *n* = 300, from three independent experiments. (E) Multiple microtubule nucleation sites, associated with C1-GFP (yellow arrows), form after nocodazole washout, which indicates that disengaged short centrioles organize functional PCM. Error bars represent the means and SD.

appendages on younger centrioles, thus eliminating the age difference among the centrioles within one cell. Inhibition of endogenous Plk1 during a centriole's second cell cycle prevented its appendage assembly during ensuing G1. Inhibition of Plk1, however, did not prevent association of appendage proteins and appendage reassembly during G1 on already mature MCs.

Results and discussion

Expression of active Plk1 in Emi1-depleted cells induces disengagement of short DCs

To analyze the effect of Plk1 activity on the maturation of short nascent centrioles, we depleted anaphase-promoting complex/cyclosome inhibitor Emi1 in a population of U2OS cells. Emi1

depletion at the beginning of the cell cycle causes the cells to continuously increase DNA content without dividing (Di Fiore and Pines, 2008; Lončarek et al., 2010; Hatano and Sluder, 2012). In such cells, the endogenous Plk1 levels are undetectable, and the cells harbor two MCs, each engaged to a 100-nm-long immature DC (Fig. S1). Therefore, Emi1-depleted (Emi1-d) cells are an ideal model to study the effect of Plk1 on centriole maturation in isolation from cell cycling. We have previously found that phosphorylation of residue T210 of Plk1 is necessary for centriole disengagement during interphase arrest. Thus, we engineered the cells to express doxycycline (dox)-inducible constitutively active T210D mutant of Plk1 (Plk1TD) at near-physiological levels (Fig. S1 and Video 1). Several hours after Plk1TD expression, centrioles in Emi1-d cells begin to disengage followed by their reduplication (Fig. S1).

DCs normally disengage in mitosis after they are almost fully elongated (Vorobjev and Chentsov, 1982). To first answer whether Plk1 induces elongation of DCs before their disengagement, Emi1-d Plk1TD-expressing cells with newly disengaged centrioles were analyzed by EM. This analysis surprisingly revealed the presence of two ∼220-nm-long disengaged DCs in the vicinity of two full-length MCs (Fig. 1 A), meaning that short DCs disengaged before reaching full length. Disengaged DCs, however, were longer than the ones from the diplosomes of Plk1-negative cells (Fig. S1; Lončarek et al., 2010), indicating that Plk1 stimulates centriole elongation.

Disengaged short centrioles in Emi1-d Plk1TD-expressing cells gradually acquire features of mature centrioles

To investigate whether disengaged short DCs further biochemically and structurally mature, we fixed Emi1-d cells at various time points after Plk1TD induction and analyzed the centrioles for the presence of mother- or daughter-specific markers by immunolabeling and EM. Immunolabeling analysis is summarized in Table S1. Sas6, a DC cartwheel protein (Strnad et al., 2007), and Centrobin, a protein that colocalizes with DCs from initiation of their formation until their duplication and is proposed to promote their elongation and stability (Zou et al., 2005; Gudi et al., 2011), were gradually lost from disengaged centrioles (Fig. 1 B and Table S1). Loss of Centrobin sometimes coincided with the presence of new C1 (centrin1)-GFP and Sas6 signals associated with disengaged DCs, indicating their duplication (Fig. 1 B, 70 h). Cep152, which mediates the recruitment of Plk4 at the centriole promoting centriole duplication (Blachon et al., 2008; Cizmecioglu et al., 2010; Hatch et al., 2010), accumulated on DCs after their disengagement (Fig.1, B and D). Loss of Sas6 and Centrobin and accumulation of Cep152 occur on disengaged DCs of cycling cells during their first G1 as a part of their maturation process. Therefore, as in cycling cells, disengaged centrioles in Emi1-d Plk1TD-expressing cells continue to mature but within the same cell cycle they were born. In addition, all disengaged centrioles were associated with various amounts of PCM proteins (Table S1) and could nucleate microtubules after nocodazole washout (Fig. 1 E). In cycling cells, only the oldest MC harbors appendage proteins Cep164 and Odf2 (Nakagawa et al., 2001; Donkor et al., 2004; Graser et al., 2007). Intriguingly, in Emi1-d cells expressing Plk1TD, both MCs and a portion of disengaged DCs were associated with these proteins (Fig. 1, C and D).

Next, we analyzed Emi1-d Plk1TD-expressing cells 70 h after Emi1 depletion (46 h after Plk1TD induction) by correlative light and EM (CLEM). This analysis revealed the presence of several generations of centrioles in the cells. The original two ∼500-nm-long MCs were found, either single or reduplicated (Fig. 2, A–C). Disengaged DCs had a mean length of ∼300 nm, which is a typical length for DCs in S-arrested cells. Although short, some of them were duplicated (Fig. 2, C and E). The ∼300-nm mean length of disengaged DCs was, however, significantly greater than the 220-nm length of freshly disengaged DCs from early time points (Fig. 1 A). Furthermore, centrioles still associated with their parent centrioles were on average ∼20% longer than procentrioles observed in control Emi1-d cells in which Plk1TD was not induced (Fig. 2 D and Fig. S1). These observations suggest that Plk1 promotes elongation of DCs. In addition, both of the longest centrioles were decorated with both sets of appendages (Fig. 2 B), and a subset of disengaged short DCs harbored appendage-like structures situated toward their distal ends, some associated with the ends of microtubules (Fig. 2 E).

Overall, the aforementioned data showed that short human centrioles can mature and perform functions associated with their proximal ends such as organization of PCM, duplication, and microtubule nucleation. In addition, the data suggested that Plk1 promotes appendage assembly and elongation of young centrioles. So, we decided to explore these novel potential roles of Plk1 in hydroxyurea (HU)-arrested and cycling cells to rule out the possibility that the observed phenotype is specific to Emi1-d cells.

Plk1 promotes premature recruitment of appendage proteins on the centrioles in HU-arrested and cycling cells

To analyze the effect of Plk1 expression on accumulation of appendage proteins on centrioles in S-arrested cells, we treated HeLa cells in G1 with HU. 18 h later, when the cells contained two MCs engaged to a ∼300-nm DC, we induced Plk1TD. Expression of Plk1TD resulted in rapid association of appendage proteins with younger MCs and with DCs after their disengagement (Fig. 3, A and B). Finally, we induced expression of Plk1TD in a population of cycling cells in early S. 48 h later, ∼50% of Plk1TD-expressing cells already harbored two or more Cep164- and Odf2-positive centrosomes (Fig. 3 C). A G2 or G1 cell with only two centrosomes, but with two or more Cep164 or Odf2 signals, indicates that centrioles born one or two cell cycles before have already biochemically matured.

To test whether centrioles with prematurely accumulated appendage proteins harbor functional appendages, we tested their ability to form cilia. We induced Plk1TD expression in MCF10A cells by dox and analyzed the cells for the presence of multiple cilia 40, 48, and 60 h later. Under control conditions, 4–7% of cycling MCF10A cells form a primary cilium (Yuan et al., 2010). Already 40 h after treatment with dox, the number of cells with two cilia increased (Fig. 3, D–F), meaning that centrioles born

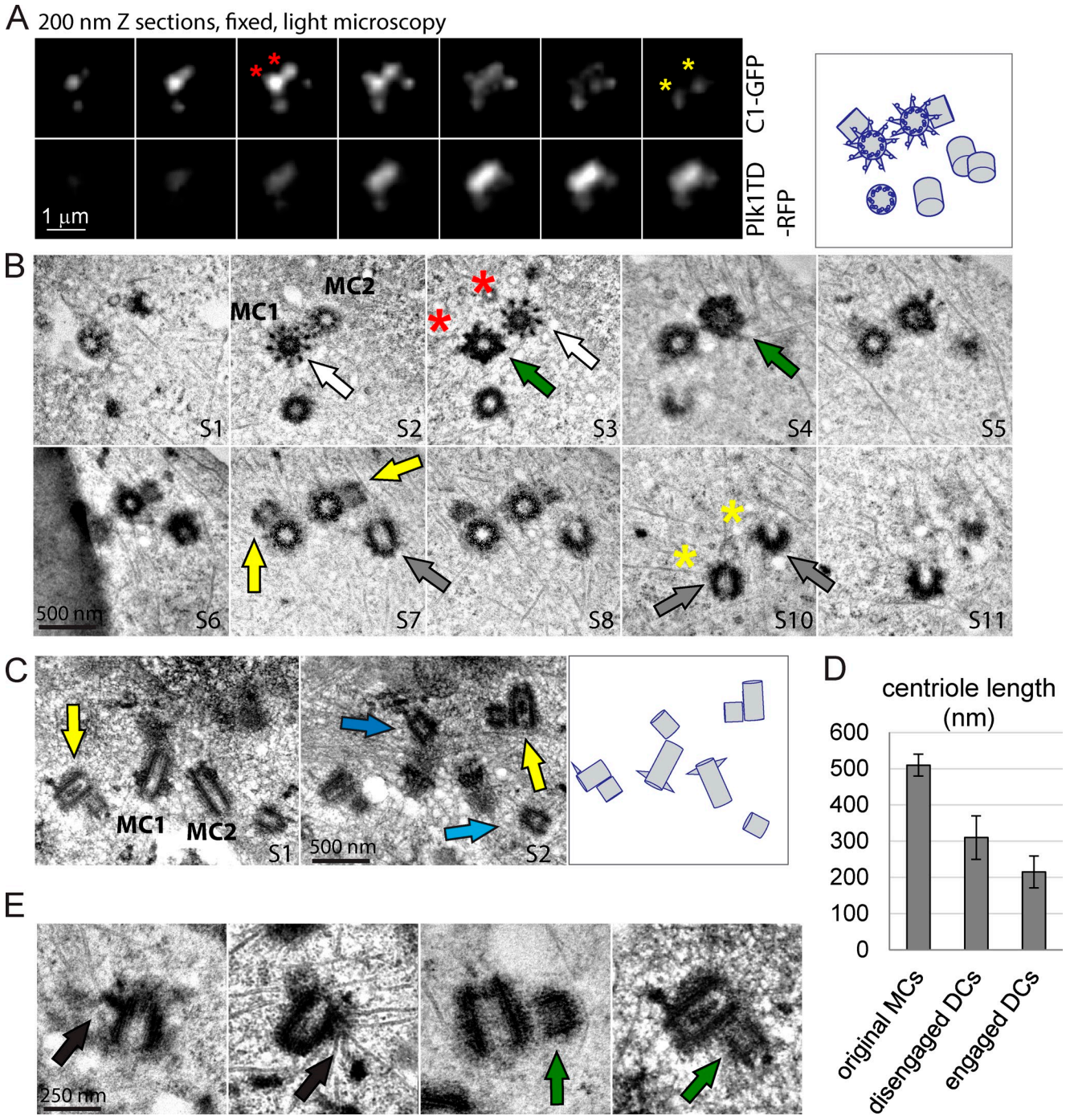

Figure 2. **CLEM analysis of centrioles in Emi1-d Plk1TD-expressing cells 70 h after Emi1 depletion and 46 h after Plk1TD expression cells that were fixed and analyzed by EM.** (A) 200-nm-thick z sections through centrosomal content of the cell. (B) EM analysis of the cell from A: two ∼500-nm-long MCs are in cross section through eight 80-nm-thick sections (S1–S8). Both MCs are associated with distal (white arrows) and subdistal (green arrows) appendages, and with a short DC (yellow arrows). Disengaged short DCs are marked with gray arrows. Red and yellow asterisks mark the same centrioles, for easier comparison of sections between A and B. (C) Two serial sections show several generations of centrioles; original MCs are sectioned longitudinally. Shorter disengaged DCs are unduplicated (blue arrows) or associated with a procentriole (yellow arrows). (D) Mean centriole length measured from electron micrographs. Error bars represent the means and SD. (E) Selected enlarged images showing short disengaged centrioles with appendage-like structures associated with microtubules (closed arrows) or engaged with a DC (green arrows). The right centriole is the enlarged centriole from C.

one or one and a half cycles before could form cilia. Expression of a kinase-dead version of Plk1 (Plk1KD) either in cycling or HU-arrested cells did not promote premature accumulation of appendage proteins on younger centrioles nor did it facilitate centriole disengagement (Fig. S1, E and F). We conclude that Plk1 activity promotes accumulation of appendage proteins universally, regardless of experimental conditions used or the ability to progress through the cell cycle, and eliminates age difference among various generations of centrioles in one cell.

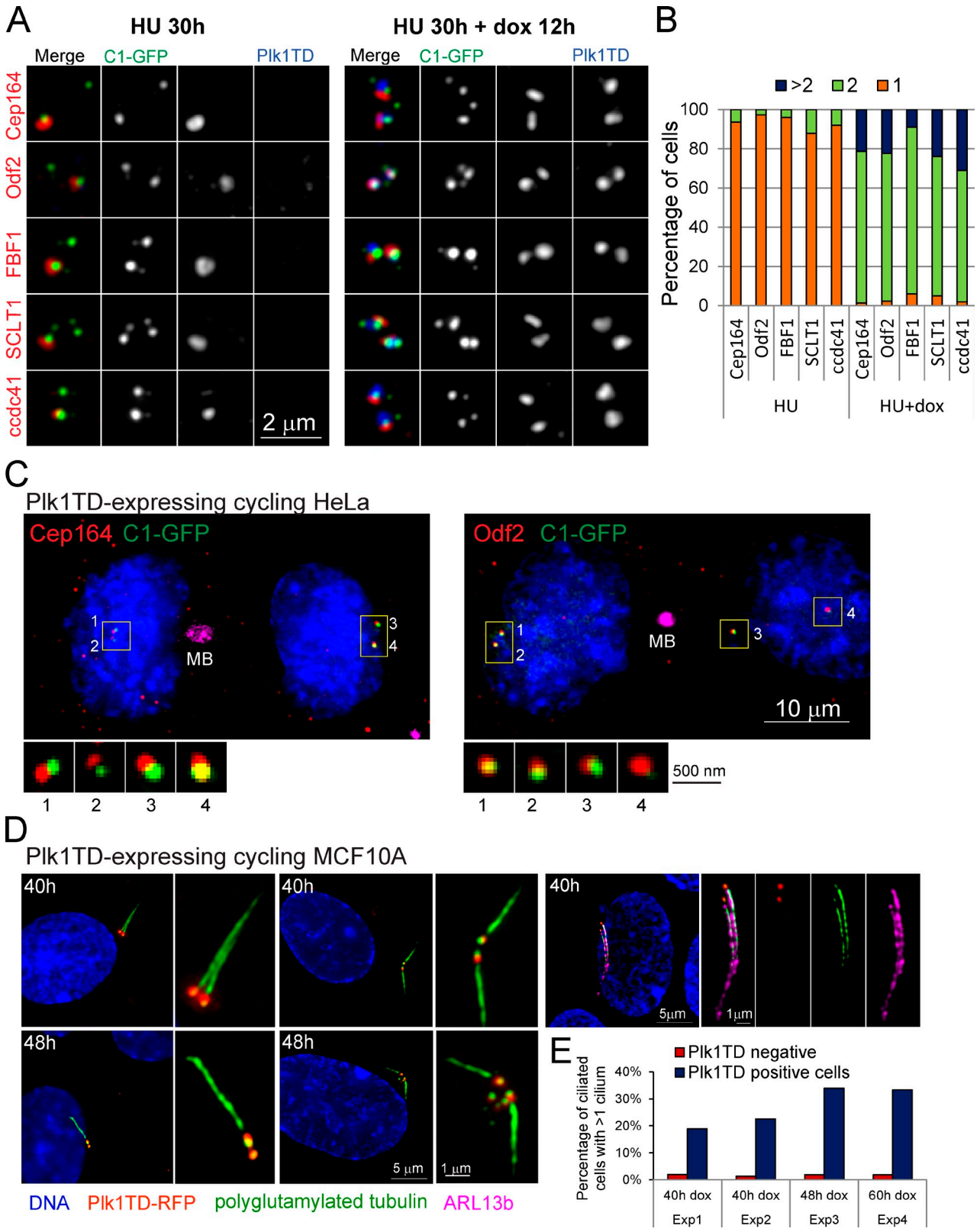

Figure 3. **Plk1 promotes premature recruitment of appendage proteins on the centrioles in HU-arrested and cycling cells.** (A) HeLa cells arrested in S phase by HU contain only one centriole associated with appendage proteins Cep164, Odf2, FBF1, SCLT1, and ccdc41. Expression of Plk1TD results in accumulation of these proteins on the other MC. (B) Quantification of the data presented in A. $n = 300$, from three independent experiments. (C) Two G1 cells expressing Plk1TD with all centrosomes associated with Cep164 (left) and Odf2 (right). Plk1TD is still visible on the midbody (MB) but degraded from the centrioles. (D) Examples of Plk1TD-expressing MCF10A cells with one or two cilia labeled for polyglutamylated tubulin and ciliary membrane protein ARL13b. (E) Percentage of ciliated cells with one or more cilia in Plk1TD-negative and -positive cells. $n \geq 100$. Exp, experiment.

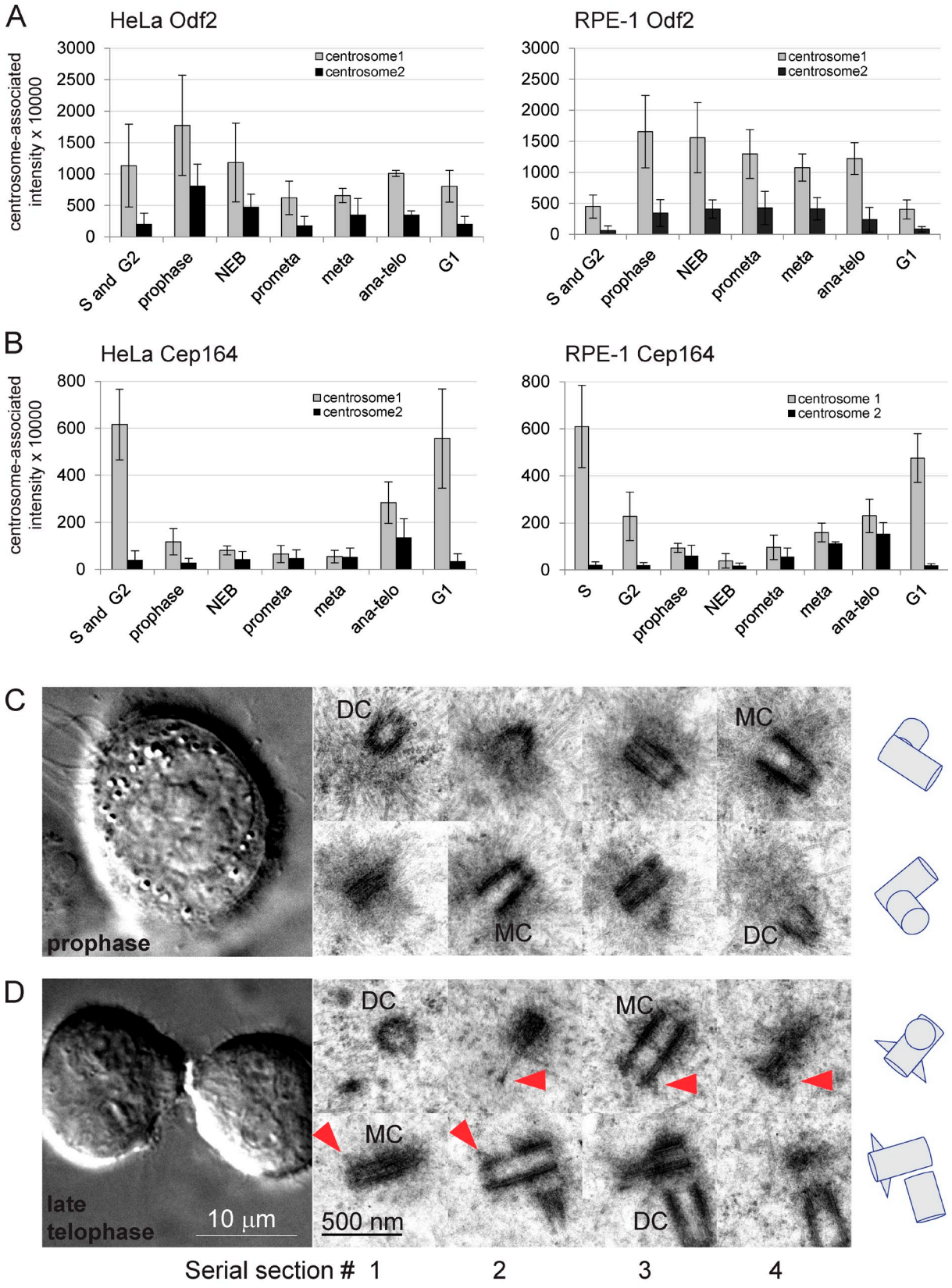

Figure 4. **Appendages are not detectable in early mitosis of HeLa cells analyzed by EM.** (A and B) Quantification of centrosome-associated Cep164 and Odf2. The error bars represent the means and SD. NEB, nuclear envelope breakdown. (C) Four serial sections of two diplosomes in prophase. Two MCs are sectioned longitudinally, and appendages are not detectable. DCs are in an oblique section. (D) Four serial sections of centrosomes in early telophase. Weak densities (arrowheads) are visible toward the distal parts of the MCs indicative of appendage reformation. meta, metaphase; ana-telo, anaphase-telophase.

Cep164 and FBF1 dissociate from the centrosomes during mitosis in a cell type–specific fashion

We hypothesized that inhibition of endogenous Plk1 in cycling cells should prevent late steps of centriole maturation and thus accumulation of appendage proteins and appendage formation on younger MCs. Two independent publications reported somewhat different dynamics of Cep164 during mitosis. Cep164 was found associated with the centrioles throughout mitosis in U2OS cells (Graser et al., 2007), whereas it was almost undetectable on mitotic centrosomes of RPE-1 cells (Schmidt et al., 2012). These differences could reflect a cell type–specific regulation of appendage proteins. So, we first characterized the dynamics of centrosome-associated Odf2, Cep164, SCLT1, ccdc41, and FBF1 during mitosis in the HeLa and RPE-1 cells we used in this study. Odf2 was associated with one MC throughout the cell cycle (Fig. 4 A). Its centrosome-associated level was the highest during prophase, when its association with the other MC was also first detected. In RPE-1 cells, higher levels of Odf2 were detected in mitosis than in interphase. SCLT1 and ccdc41 dynamics were similar to Odf2, both in HeLa (Fig. S2) and RPE-1. Contrary to Odf2, centrosome-associated Cep164 showed drastic fluctuations during mitosis (Fig. 4 B). In S and G2, Cep164 was associated with only one centrosome. In prophase, Cep164 fluorescence intensity decreased 20-fold in comparison to interphase and sometimes was reduced to background levels after nuclear envelope breakdown. From anaphase to G1, the intensity of Cep164 steadily increased along with its recruitment onto the other MC. Likewise, centrosome-associated FBF1 levels were drastically diminished or undetectable in ∼80% of HeLa cells during early stages of mitosis (Fig. S2) but not from RPE-1 cells, in agreement with a previous study (Tanos et al., 2013).

Cep164 and FBF1 are necessary for the assembly of distal appendages and ciliogenesis (Graser et al., 2007; Tanos et al., 2013). Therefore, we asked whether their temporary dissociation from mitotic centrosomes results in disintegration of appendages in early mitosis. We analyzed the centrosomes of HeLa and RPE-1 cells in mitosis by EM (n = 8). Appendages were not detected on either MC in prophase and prometaphase (Fig. 4 C). After metaphase, however, we detected structures of higher densities on both MCs at the sites where appendages would normally be located (Fig. 4 D), in agreement with previous findings in HeLa cells (Robbins et al., 1968). Thus, we conclude that in HeLa cell appendages disassemble, or at least drastically modify, upon mitotic entry and reassemble by the end of mitosis, in parallel with fluctuation in the level of centriole-associated Cep164 and FBF1. Contrary to our findings, distal appendages persist through mitosis in association with a ciliary vesicle in mouse embryonic neocortical stem cells and HEK293T and Neuro2a cells (Paridaen et al., 2013). Also, in pig kidney embryo cells, distal appendages were detected already in metaphase on older MCs and during anaphase on younger MCs (Vorobjev and Chentsov, 1982). Collectively, these data signify cell type–specific regulation of appendage dynamics.

Inhibition of Plk1 during S and G2 prevents appendage formation on young MCs in after G1

Next, we analyzed the consequences of endogenous Plk1 inhibition on appendage assembly. We inhibited Plk1 with BI 2536 (BI; Lénárt et al., 2007), collected mitotic cells 12 h later, and then drove the cells into G1 by inhibiting Cdk1/Cyclin B activity with RO-3306 inhibitor (RO; Vassilev et al., 2006). 3 h later, we analyzed the centrosomes in these tetraploid G1 cells (G1BIRO) for the presence of appendage proteins. Control cells obtained by treating a mitotic population with RO only (G1RO) contained ∼96% of the cells with two Cep164-, FBF1-, SCLT1-, and ccdc41-positive centrosomes. Contrary to this, in G1BIRO cells (Fig. 5, A and B), the centrioles stayed engaged with only one diplosome associated with a signal. EM analysis of G1BIRO cells revealed the presence of appendages on only one of the diplosomes in 12 out of 12 analyzed cells (Fig. 5 C).

We then analyzed the accumulation of appendage proteins on G1 centrosomes as a function of various durations of Plk1 inhibition in the proceeding cell cycle. We collected mitotic cells at increasing time points after Plk1 inhibition and then drove the cells into G1. 2 h later, we analyzed the centrosomes for the presence of appendage proteins. In control untreated samples, all G1 cells contained either two signals of equal or of slightly different brightness (Fig. 5 D). However, with increasing duration of Plk1 inhibition, the percentage of cells with two signals steadily decreased. Therefore, Plk1 activity through S and G2 allows the younger MC to acquire the final biochemical modifications required for accumulation of appendage proteins in the subsequent cell cycle. This result signifies that centriole maturation is not just a function of centriole age but that it is dependent on some Plk1-dependent processes during mid-S and G2 of the centriole's second cell cycle. Interestingly, in G1BIRO cells, neither accumulation of appendage proteins nor appendage assembly on the older MCs that have matured in earlier cell cycles was affected by Plk1 inhibition, meaning that once the centrioles fully matured, they retained the ability to form appendages.

Plk1 activity is necessary for elongation of DCs in HU-arrested and cycling cells

Finally, we directly tested a role for Plk1 in elongation of DCs in HU-arrested and cycling cells. EM analysis of centriole length in Emi1-d Plk1TD-expressing cells (Fig. 2) suggested that Plk1 activity promotes DC elongation. First, we induced Plk1TD in HU-arrested cells and, 20 h later, labeled the cells for Sas6. We calculated the distance between Sas6 and DC-associated C1-GFP, as an indicator of centriole length (Fig. 5 E). In HU-arrested cells, the mean distance between the Sas6 and C1-GFP signals was ∼190 nm. After Plk1TD expression, this distance increased to ∼320 nm, indicating that the centrioles elongated. To evaluate how inhibition of endogenous Plk1 affects centriole elongation in cycling cells, we prepared G1BIRO cells (see previous paragraph) and measured the distance between Sas6 and C1-GFP. Untreated cells in prophase with a mean Sas6–C1-GFP distance of 300 nm were used as controls. In cells with endogenous Plk1 inhibited from S to the ensuing G1, Sas6 to C1-GFP distance was 210 nm, meaning that in the absence of Plk1, DCs

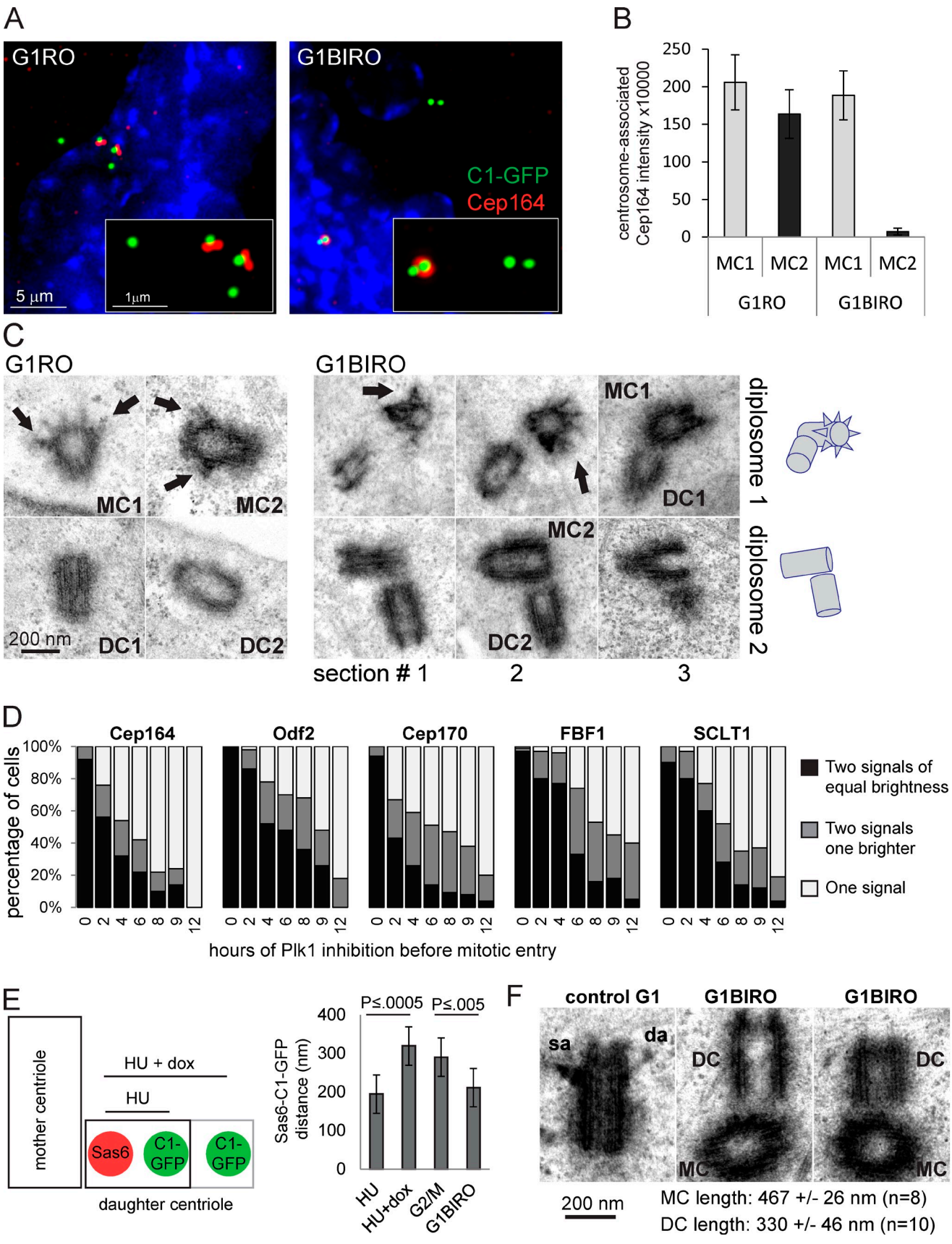

Figure 5. **Plk1 inhibition prevents appendage formation on young MCs and elongation of DCs.** (A) Detection of centrosome-associated Cep164 by immunolabeling. In control G1RO cells, obtained by treating mitotic cells with Cdk1 inhibitor RO, Cep164 associates with two centrioles (marked by C1-GFP). In G1RO-treated mitotic cells, pretreated with Plk1 inhibitor BI for 12 h (G1BIRO), Cep164 associates with one MC. (B) Quantification of Cep164 signals from A.

did not elongate beyond their original length in S. EM analysis of G1BIRO cells confirmed that DCs were on average 30% shorter than fully grown centrioles, (Fig. 5 F). Therefore, Plk1 is necessary for elongation of DCs in cycling cells.

Conclusions and implications

Our data suggest that controlled Plk1 activity during two consecutive cell cycles is necessary for timely centriole maturation. Unscheduled Plk1 activity accelerates maturation of nascent centrioles and eliminates necessary biochemical and structural differences between three generations of centrioles (Fig. S3). These differences are necessary to ensure that only one centriole is competent for ciliogenesis, but two are competent for duplication and centrosome assembly in cycling cells. Our findings reveal two novel functions of Plk1 on the centrosome, in regulation of appendage dynamics and centriole elongation, providing better insights into centriole cycle.

Materials and methods

Cell lines

HeLa, U2OS, and RPE-1 cells with cytomegalovirus-driven constitutive expression of Centrin-GFP were described previously (Piel et al., 2000; Lončarek et al., 2008, 2010). In brief, pEGFP-N1 vector (Takara Bio Inc.) was used to express a full-length Centrin-GFP cDNA in HeLa cells, and Lentilox3.1 vector was used for Centrin-GFP expression in RPE-1 and U2OS cells. The cells were cultured in DMEM (Invitrogen) supplemented with 10% fetal calf serum and 1% penicillin/streptomycin. MCF10A cells (ATCC) were maintained in DMEM supplemented with 0.1 µg/ml cholera toxin (EMD Millipore), 0.5 µg/ml hydrocortisone (Sigma-Aldrich), 10 µg/ml insulin, 0.02 µg/ml EGF (EMD Millipore), 5% horse serum (Invitrogen), and 1% penicillin/streptomycin. All cells were grown at 37°C in a humidified atmosphere of 5% CO_2. For live-cell imaging, cells grown on the coverslips were assembled into Rose chambers and perfused with complete CO_2-independent medium (Invitrogen).

Plasmid constructs and lentiviral transfection

An ERFP coding sequence without its stop codon was amplified by PCR and ligated into the pLVX-TRE3G vector (Takara Bio Inc.) using restriction enzymes BamHI and ApaI, generating pLVX-TRE3G-RFP. Full-length cDNA of constitutively active T210D mutant of Plk1 (Plk1TD) was amplified by PCR from the plasmid pQE-80L-Plk1T210D (gift from C. Bieberich, University of Maryland, Baltimore, MD) using 5′-ACGGGGCCCATGAGTGCTGCAGTGACTGCAGG-3′ as a forward and 5′-ACGACGCGTTTAGGAGGCCTTGAGACGGTTGC-3′ as a reverse primer. cDNA was then ligated into pLVX-TRE3G-RFP vector using restriction enzymes ApaI and MluI, generating an inducible Plk1TD-RFP fusion expression cassette. Lentiviruses carrying a Tet3G or Plk1TD-RFP expression cassette were generated according to the manufacturer's instructions. The target cells were infected, and stable clones were selected in media containing 2 µg/ml puromycin and 800 µg/ml G418. The expression of Plk1TD-RFP fusion protein in resistant cells was induced by 1 µg/ml dox. pUHD-YFP-Plk1-KD (825) carrying the K82R mutation (39874; Addgene; deposited by J. Pines, Wellcome Trust/Cancer Research UK Gurdon Institute Cambridge, Cambridge, England, UK; Mundt et al., 1997) was used to express a kinase-dead mutant of Plk1 (Plk1KD). The plasmid was transfected using Lipofectamine transfection reagent (Invitrogen) following the manufacturer's instructions.

Cell treatment and siRNA transfection

To prepare Emi1-d cells, mitotic U2OS or HeLa cells were collected by shake off from logarithmically growing populations and plated on coverslips. 1.5 h later, the cells were transfected with Emi1 siRNA (5′-ACTTGCTGCCAGTTCA-3′; synthesized by Thermo Fisher Scientific) using Oligofectamine (Invitrogen) following the manufacturer's instructions. 22 h after transfection (by that time most of the cells were already endocycling, judging by the lack of mitosis and growing nuclei), some cultures were treated with dox, to induce Plk1TD expression. Cultures without dox were used as controls. Live-cell video microscopy, when needed, was initiated several hours after dox treatment, and the cells were fixed for immunostaining or CLEM analysis 24–48 h after dox treatment (corresponding to the 46 and 70 h after Emi1 depletion, respectively).

To prepare S phase–arrested cells, mitotic cells were shaken off, plated on a coverslip, and 2 h later, treated with 2 mM HU. Plk1TD expression was induced by dox 24 h after the shake off. The cells were fixed and analyzed by immunofluorescence or by CLEM, as required.

To analyze the effect of Plk1 on centriole elongation, mitotic cells were shaken off, plated on the coverslips, and 6 h later, treated with 200 nM of specific Plk1 inhibitor BI. Cells with inhibited Plk1 entered mitosis and arrested in prometaphase. 1 h after mitotic arrest, mitotic cells were harvested and treated with 9 µM of Cdk1 inhibitor RO to promote mitotic exit. 3 h later, the cells were fixed, immunostained for Sas6 for light microscopy analysis, or fixed with glutaraldehyde for CLEM. As controls, we used mitotic cells treated with RO only. Cycling cells with visible signs of chromatin condensation (G2/M) were used as an additional control in measuring of centriole length.

To analyze the effect of Pk1 on recruitment of appendage proteins and appendage assembly on the centrosomes of postmitotic cycling cells, logarithmically growing cells were treated with Plk1 inhibitor BI. 12 h later, mitotic cells were collected and treated with RO. Postmitotic cells were fixed 3 h later, immunolabeled, analyzed for the presence of Cep164, Odf2, Cep170, SCLT1, and FBF1 on the centrosomes, and analyzed by light microscopy or fixed by 2.5% glutaraldehyde for CLEM.

To analyze how accumulation of appendage proteins to the centrosomes of postmitotic cells is affected by various durations of Plk1 inhibition in the proceeding cell cycle, logarithmically growing cells were treated with BI. Mitotic cells were then collected 2, 4, 6, 8 10, and 12 h later and treated with RO. 2 h later, the cells were fixed, immunolabeled, and analyzed for the presence of Cep164, Odf2, Cep170, SCLT1, and FBF1.

Immunostaining

Cells were grown on the coverslips, treated as needed, fixed with 1.5% formaldehyde in PBS for 5 min, and postfixed with cold methanol for 5 min at −20°C. After rehydration, cells were blocked in 1% BSA and 0.05% Tween 20 in PBS and incubated with primary antibodies. Various fluorescence-labeled secondary antibodies (Invitrogen) were used to visualize the proteins. DNA was stained with Hoechst 33342 (Invitrogen). The following primary antibodies were used for immunostaining in this study: mouse monoclonal anti-Sas6 (sc-81431; Santa Cruz Biotechnology, Inc.) at 1:500, mouse monoclonal anti–γ-tubulin (T6557; Sigma-Aldrich) at 1:1,000, mouse anti-Centrobin (ab70448; Abcam) at 1:600, rabbit anti-Odf2/Cenexin (12058-1-AP; Proteintech) at 1:500, rabbit anti-Cep170 (IHC-00265; Bethyl Laboratories, Inc.) at 1:500, goat anti-Cep164 (sc-240226; Santa Cruz Biotechnology, Inc.) at 1:700, rabbit anti-hPOC5 (a gift from J. Azimzadeh, Institute Jacques Monod, Paris, France) at 1:1,000, mouse anti–polyglutamylated tubulin (GT335 and T9822; Sigma-Aldrich) at 1:1,000, mouse monoclonal anti–α-tubulin (T9026; Sigma-Aldrich) at 1:700, TRITC-conjugated anti–γ-tubulin (sc-7396; Santa Cruz Biotechnology, Inc.) at 1:200, rabbit anti-Cep152 (A302-479A; Bethyl Laboratories, Inc.) at 1:4,000, mouse anti-ARL13B (17711-1-AP; Proteintech) at 1:300, rabbit anti-SCLT1 (HPA036561; Sigma-Aldrich) at 1:200, rabbit anti-FBF1 (HPA023677; Sigma-Aldrich) at 1:200, and rabbit anti-ccdc41 (HPA038161; Sigma-Aldrich) at 1:200. Anti-Cep120 antibodies were

The error bars represent the means and SD. (C) CLEM analysis of cells obtained as described in A. (left) Appendages are detectable on two disengaged centrioles (arrows). (right) Three serial sections through the diplosomes of G1BIRO cell. Only one MC is associated with appendages (arrows). (D) Plk1 inhibitor was added to a population of cycling cells. Cells entering mitosis after increasing duration of Plk1 inhibition were collected, driven out of mitosis, and immunolabeled, and the number of Cep164, Odf2, Cep170, FBF1, and SCLT1 signals per cell was scored. (E) Distance between proximal Sas6 and C1-GFP signals increases in HU-arrested cells after induction of Plk1TD. In G1BIRO cells, the distance between Sas6 and C1-GFP is not significantly different from that in HU-treated cells, suggesting that inhibition of endogenous Plk1 prevents elongation of DCs during G2 and M. (F) DCs in G1BIRO cells are, on average, 30% shorter than their MCs. (left) A representative ∼470-nm MC with distal (da) and subdistal (sa) appendages from the G1 cell. (middle and right) Two examples of G1BIRO diplosomes with DCs shorter than an average control centriole.

provided by M. Mahjoub (Washington University School of Medicine, St. Louis, MO) and used at a 1:400 dilution.

Light microscopy

Wide-field fluorescence microscopy was performed on an inverted microscope (Eclipse Ti; Nikon), equipped with a 64-µm-pixel camera (CoolSNAP HQ^2; Photometrics) and illuminator (Intensilight; Nikon), using 100× Plan Apochromat NA 1.42 or 60×, NA 1.45 Plan Apochromat total internal reflection fluorescence (TIRF) objective, with or without a 1.5× magnifying lens. Images were captured using NIS-Elements (Nikon) imaging software, and 3D deconvolution was performed by AutoQuant X3 software (Media Cybernetics). For image assembly, we used ImageJ (National Institutes of Health) and NIS-Elements. For live-cell imaging, cells growing on the coverslip were assembled into the Rose chambers and imaged by inverted microscope (Eclipse Ti) enclosed in an environmental chamber at 37°C, equipped with a spinning-disk confocal (CSUX Spinning Disk; Yokogawa Electric Corporation) and a back-illuminated 16-µm-pixel electron-multiplying charge-coupled device camera (DU897; Andor Technology). 100×, NA 1.42 Plan Apochromat or 60×, NA 1.45 Plan Apochromat TIRF objective lenses were used in conjunction with a 1.5× magnifying lens.

CLEM

For CLEM analysis, cells in Rose chambers were imaged on a confocal microscope. Rose chambers were then perfused with 2.5% glutaraldehyde, and 200-nm-thick z sections through the entire cell volume were recorded to register the position of the centrioles in the cells. The position of the cells on the coverslip was then marked by a diamond scribe. Rose chambers were disassembled, and the cells were washed in PBS for 30 min followed by dehydration and staining with osmium tetroxide and uranyl acetate, after which the cells were embedded in Embed 812 resin. The same cell identified by light microscopy was then serially sectioned. 80-nm-thick serial sections were transferred onto copper slot grids, stained with uranyl acetate and lead citrate, and imaged using a transmission electron microscope (H-7650; Hitachi). Image analysis and section alignment were performed in Photoshop (Adobe) and ImageJ. The length of the centrioles was measured from electron micrographs in ImageJ. Only centrioles sectioned in longitudinal or almost longitudinal orientation were measured.

Measurement of centriole length by light microscopy

To estimate the distance between various fluorescence signals in 3D volume (used to measure centriole length by light microscopy; Fig. 5), we used classical wide-field fluorescence or structural illumination microscope (N-SIM; Nikon), with similar results. Plk1TD-expressing cells were fixed and immunolabeled for Sas6 to mark the proximal ends of DCs. The z series spanning entire cells were then collected (voxel size for wide field was 43 × 43 × 200 nm, and for SIM, the size was 31 × 31 × 100 nm), and the center of mass for each C1-GFP and Sas6 signal was manually determined directly from z series. Extracted 3D coordinates of individual signals were then used to calculate the distance between two signals in Excel (Microsoft) by using 3D Pythagorean theorem (for details please see Supplemental material). To correct for xyz chromatic shift, 100-nm fluorescent blue/green/orange/dark red microspheres (TetraSpek; Invitrogen) were added to the mounting medium for calibration. 3D distribution of the signals of TetraSpek in different channels was used for channel alignment of the images before extraction of 3D coordinates of individual signals. For channel alignment, we used an NIS-Elements macro written by R. Gruskin and S. Kiriyama from the Nikon Software Department (Melville, NY; Macro is available on request to all NIS-Elements users). Using this strategy, a local xyz correction was applied for each centrosome, eliminating inconsistencies originating in variability of coverslip thickness or chromatic shift caused by the random distance of the centrosomes from the coverslip surface, which both may decrease the accuracy of the measurement. 20 centrosomes per dataset were measured.

Fluorescence intensity measurement

Quantification of centrosome-associated fluorescence intensity of Cep164 and Odf2 and FBF1 for Fig. 4 and Fig. S2 was performed using ImageJ. The centrosomes were identified by C1-GFP signals. Integrated density of centrosome-associated proteins was measured from the summed intensity projections of z stacks. Integrated density was measured from a defined area of a constant size encircling the centrosome. Intensity of the background in a near proximity of each centrosome was subtracted from the signal intensity. At least 20 centrosomes were measured for each cell cycle phase.

Immunoblotting

Cells were lysed directly in SDS loading buffer, samples were syringed, boiled, and run on 10% polyacrylamide gels. Proteins were transferred to a nitrocellulose membrane. Membrane was blocked in 3% milk and incubated with primary antibody for 1 h at room temperature or overnight at 4°C and then with horseradish peroxidase–conjugated secondary antibodies (1:10,000; GE Healthcare), and the signal was detected using a detection system (Bio-Rad Laboratories) according to the manufacturer's instructions. The following primary antibodies used for Western blotting were mouse monoclonal anti-Plk1 (sc-17783; Santa Cruz Biotechnology, Inc.) at 1:500, mouse monoclonal anti-Emi1 (37-6600; Invitrogen) at 1:100, and mouse monoclonal anti–α-tubulin (T9026) at 1:1,000.

Determination of statistical significance

The statistical difference between two datasets was determined using *t* test for two paired samples by Excel Analysis Toolpak. P-values (two tail) <0.05 were considered to be significantly different.

Online supplemental material

Fig. S1 describes the effect Plk1TD-RFP expression in Emi1-d cells and compares the levels of endogenous and induced Plk1 under various experimental conditions. Fig. S2 illustrates the dynamics of centrosome-associated appendage proteins SCLT1, ccdc41, and FBF1 throughout mitosis. Fig. S3 is a graphical abstract summarizing the effects of Plk1 inhibition and expression on the centriole cycle in cycling cells and interphase-arrested cells. Table S1 lists centrosomal proteins analyzed by immunofluorescence in Emi1-d cells and summarizes their dynamics on the centrioles before and after induction of Plk1TD expression. Video 1 shows that almost physiological level of Plk1TD-RFP in the cells is undergoing a typical cell cycle–dependent degradation and relocalization to the different cellular structures (kinetochores, centrosomes, and midbody). Supplemental material also includes an Excel file that shows a distance calculator for multichannel 3D images used in this study. Online supplemental material is available at http://www.jcb.org/cgi/content/full/jcb.201407087/DC1.

We thank members of Electron Microscopy Core at Advanced Technology Research Facility in Frederick for assistance with the transmission EM microscope and Drs. Allan Weissman, Alexey Khodjakov, Monica Bettencourt-Dias, and Michael Kuehn for discussions and critical reading of the manuscript.

This research was supported by the Intramural Research Program of the National Institutes of Health, National Cancer Institute, Center for Cancer Research.

The authors declare no competing financial interests.

Submitted: 22 July 2014
Accepted: 18 August 2014

References

Blachon, S., J. Gopalakrishnan, Y. Omori, A. Polyanovsky, A. Church, D. Nicastro, J. Malicki, and T. Avidor-Reiss. 2008. *Drosophila* asterless and vertebrate Cep152 Are orthologs essential for centriole duplication. *Genetics*. 180:2081–2094. http://dx.doi.org/10.1534/genetics.108.095141

Cizmecioglu, O., M. Arnold, R. Bahtz, F. Settele, L. Ehret, U. Haselmann-Weiss, C. Antony, and I. Hoffmann. 2010. Cep152 acts as a scaffold for recruitment of Plk4 and CPAP to the centrosome. *J. Cell Biol.* 191:731–739. http://dx.doi.org/10.1083/jcb.201007107

Di Fiore, B., and J. Pines. 2008. Defining the role of Emi1 in the DNA replication-segregation cycle. *Chromosoma*. 117:333–338. http://dx.doi.org/10.1007/s00412-008-0152-x

Donkor, F.F., M. Mönnich, E. Czirr, T. Hollemann, and S. Hoyer-Fender. 2004. Outer dense fibre protein 2 (ODF2) is a self-interacting centrosomal protein with affinity for microtubules. *J. Cell Sci.* 117:4643–4651. http://dx.doi.org/10.1242/jcs.01303

Graser, S., Y.-D. Stierhof, S.B. Lavoie, O.S. Gassner, S. Lamla, M. Le Clech, and E.A. Nigg. 2007. Cep164, a novel centriole appendage protein required for primary cilium formation. *J. Cell Biol.* 179:321–330. http://dx.doi.org/10.1083/jcb.200707181

Guarguaglini, G., P.I. Duncan, Y.D. Stierhof, T. Holmström, S. Duensing, and E.A. Nigg. 2005. The forkhead-associated domain protein Cep170 interacts with Polo-like kinase 1 and serves as a marker for mature centrioles. *Mol. Biol. Cell*. 16:1095–1107. http://dx.doi.org/10.1091/mbc.E04-10-0939

Gudi, R., C. Zou, J. Li, and Q. Gao. 2011. Centrobin–tubulin interaction is required for centriole elongation and stability. *J. Cell Biol.* 193:711–725. http://dx.doi.org/10.1083/jcb.201006135

Hatano, T., and G. Sluder. 2012. The interrelationship between APC/C and Plk1 activities in centriole disengagement. *Biol. Open*. 1:1153–1160. http://dx.doi.org/10.1242/bio.20122626

Hatch, E.M., A. Kulukian, A.J. Holland, D.W. Cleveland, and T. Stearns. 2010. Cep152 interacts with Plk4 and is required for centriole duplication. *J. Cell Biol.* 191:721–729. http://dx.doi.org/10.1083/jcb.201006049

Hoyer-Fender, S. 2010. Centriole maturation and transformation to basal body. *Semin. Cell Dev. Biol.* 21:142–147. http://dx.doi.org/10.1016/j.semcdb.2009.07.002

Lénárt, P., M. Petronczki, M. Steegmaier, B. Di Fiore, J.J. Lipp, M. Hoffmann, W.J. Rettig, N. Kraut, and J.-M. Peters. 2007. The small-molecule inhibitor BI 2536 reveals novel insights into mitotic roles of polo-like kinase 1. *Curr. Biol.* 17:304–315. http://dx.doi.org/10.1016/j.cub.2006.12.046

Lončarek, J., P. Hergert, V. Magidson, and A. Khodjakov. 2008. Control of daughter centriole formation by the pericentriolar material. *Nat. Cell Biol.* 10:322–328. http://dx.doi.org/10.1038/ncb1694

Lončarek, J., P. Hergert, and A. Khodjakov. 2010. Centriole reduplication during prolonged interphase requires procentriole maturation governed by Plk1. *Curr. Biol.* 20:1277–1282. http://dx.doi.org/10.1016/j.cub.2010.05.050

Mogensen, M.M., A. Malik, M. Piel, V. Bouckson-Castaing, and M. Bornens. 2000. Microtubule minus-end anchorage at centrosomal and non-centrosomal sites: the role of ninein. *J. Cell Sci.* 113:3013–3023.

Mundt, K.E., R.M. Golsteyn, H.A. Lane, and E.A. Nigg. 1997. On the regulation and function of human polo-like kinase 1 (PLK1): effects of overexpression on cell cycle progression. *Biochem. Biophys. Res. Commun.* 239:377–385. http://dx.doi.org/10.1006/bbrc.1997.7378

Nakagawa, Y., Y. Yamane, T. Okanoue, S. Tsukita, and S. Tsukita. 2001. Outer dense fiber 2 is a widespread centrosome scaffold component preferentially associated with mother centrioles: its identification from isolated centrosomes. *Mol. Biol. Cell*. 12:1687–1697. http://dx.doi.org/10.1091/mbc.12.6.1687

Paintrand, M., M. Moudjou, H. Delacroix, and M. Bornens. 1992. Centrosome organization and centriole architecture: their sensitivity to divalent cations. *J. Struct. Biol.* 108:107–128. http://dx.doi.org/10.1016/1047-8477(92)90011-X

Paridaen, J.T., M. Wilsch-Bräuninger, and W.B. Huttner. 2013. Asymmetric inheritance of centrosome-associated primary cilium membrane directs ciliogenesis after cell division. *Cell*. 155:333–344. http://dx.doi.org/10.1016/j.cell.2013.08.060

Piel, M., P. Meyer, A. Khodjakov, C.L. Rieder, and M. Bornens. 2000. The respective contributions of the mother and daughter centrioles to centrosome activity and behavior in vertebrate cells. *J. Cell Biol.* 149:317–330. http://dx.doi.org/10.1083/jcb.149.2.317

Rattner, J.B., and S.G. Phillips. 1973. Independence of centriole formation and DNA synthesis. *J. Cell Biol.* 57:359–372. http://dx.doi.org/10.1083/jcb.57.2.359

Robbins, E., G. Jentzsch, and A. Micali. 1968. The centriole cycle in synchronized HeLa cells. *J. Cell Biol.* 36:329–339. http://dx.doi.org/10.1083/jcb.36.2.329

Schmidt, K.N., S. Kuhns, A. Neuner, B. Hub, H. Zentgraf, and G. Pereira. 2012. Cep164 mediates vesicular docking to the mother centriole during early steps of ciliogenesis. *J. Cell Biol.* 199:1083–1101. http://dx.doi.org/10.1083/jcb.201202126

Strnad, P., S. Leidel, T. Vinogradova, U. Euteneuer, A. Khodjakov, and P. Gönczy. 2007. Regulated HsSAS-6 levels ensure formation of a single procentriole per centriole during the centrosome duplication cycle. *Dev. Cell*. 13:203–213. http://dx.doi.org/10.1016/j.devcel.2007.07.004

Tanos, B.E., H.-J. Yang, R. Soni, W.-J. Wang, F.P. Macaluso, J.M. Asara, and M.-F.B. Tsou. 2013. Centriole distal appendages promote membrane docking, leading to cilia initiation. *Genes Dev.* 27:163–168. http://dx.doi.org/10.1101/gad.207043.112

Tateishi, K., Y. Yamazaki, T. Nishida, S. Watanabe, K. Kunimoto, H. Ishikawa, and S. Tsukita. 2013. Two appendages homologous between basal bodies and centrioles are formed using distinct *Odf2* domains. *J. Cell Biol.* 203:417–425. http://dx.doi.org/10.1083/jcb.201303071

Tsou, M.-F.B., and T. Stearns. 2006. Controlling centrosome number: licenses and blocks. *Curr. Opin. Cell Biol.* 18:74–78. http://dx.doi.org/10.1016/j.ceb.2005.12.008

Tsou, M.-F.B., W.-J. Wang, K.A. George, K. Uryu, T. Stearns, and P.V. Jallepalli. 2009. Polo kinase and separase regulate the mitotic licensing of centriole duplication in human cells. *Dev. Cell*. 17:344–354. http://dx.doi.org/10.1016/j.devcel.2009.07.015

Vassilev, L.T., C. Tovar, S. Chen, D. Knezevic, X. Zhao, H. Sun, D.C. Heimbrook, and L. Chen. 2006. Selective small-molecule inhibitor reveals critical mitotic functions of human CDK1. *Proc. Natl. Acad. Sci. USA*. 103:10660–10665. http://dx.doi.org/10.1073/pnas.0600447103

Vidwans, S.J., M.L. Wong, and P.H. O'Farrell. 1999. Mitotic regulators govern progress through steps in the centrosome duplication cycle. *J. Cell Biol.* 147:1371–1378. http://dx.doi.org/10.1083/jcb.147.7.1371

Vorobjev, I.A., and Y.S. Chentsov. 1982. Centrioles in the cell cycle. I. Epithelial cells. *J. Cell Biol.* 93:938–949. http://dx.doi.org/10.1083/jcb.93.3.938

Yuan, K., N. Frolova, Y. Xie, D. Wang, L. Cook, Y.-J. Kwon, A.D. Steg, R. Serra, and A.R. Frost. 2010. Primary cilia are decreased in breast cancer: analysis of a collection of human breast cancer cell lines and tissues. *J. Histochem. Cytochem.* 58:857–870. http://dx.doi.org/10.1369/jhc.2010.955856

Zou, C., J. Li, Y. Bai, W.T. Gunning, D.E. Wazer, V. Band, and Q. Gao. 2005. Centrobin: a novel daughter centriole-associated protein that is required for centriole duplication. *J. Cell Biol.* 171:437–445. http://dx.doi.org/10.1083/jcb.200506185